

Stress-induced mass detection with a micromechanical/nanomechanical silicon resonator

著者	ONO Takahito, Esashi Masayoshi
journal or publication title	Review of scientific instruments
volume	76
number	9
page range	093107-1-093107-5
year	2005
URL	http://hdl.handle.net/10097/35176

doi: 10.1063/1.2041591

Stress-induced mass detection with a micromechanical/nanomechanical silicon resonator

Takahito Ono^{a)} and Masayoshi Esashi

Graduate School of Engineering, Tohoku University, Aza Aoba 6-6-01, Aramaki, Aobaku, Sendai 980-8579, Japan

(Received 29 June 2005; accepted 26 July 2005; published online 2 September 2005)

The potential ability of micromechanical/nanomechanical silicon resonators with thicknesses of 500 and 146 nm to detect mass and charge in an ion attachment is investigated in vacuum. Low-energy ions are generated by an ionizer and filtered by a quadrupole mass filter. The vibration of the resonator is measured using a laser Doppler vibrometer, which self-oscillates at its fundamental resonant frequency by feedback-controlled electrostatic actuation. The vibration amplitude is kept at a constant with the auto gain control of the feedback loop. The attachment of ions on the one side of the resonator induces the surface stress, resulting in the change of the resonant frequency. Also the feedback gain that keeps the amplitude at a constant changes due to the charge deposition. The measurement of the mass-induced stress of 9.7×10^{-7} N/m that resulted from a mass attachment smaller than 69 Zg is demonstrated using the 146-nm-thick silicon resonator. © 2005 American Institute of Physics. [DOI: 10.1063/1.2041591]

I. INTRODUCTION

Resonating mesomechanical and nanomechanical sensors increase their sensitivity and decrease the influence of thermomechanical noise by scaling down. Such scaling merits are becoming the driving force to miniaturize sensors.^{1,2} Resonating silicon sensors have been widely used as a key component for sensing a force in scanning probe microscopy (SPM).³ The minimum detectable force of atto (10^{-18}) N has been achieved with a resonating silicon sensor at a cryogenic temperature.⁴ Such a force sensor can detect various physical interactions, such as electrostatic,^{5,6} magnetic,^{7,8} chemical,^{9,10} and thermal interactions¹¹ etc., making the force sensor a versatile tool in wide fields. For example, an electrometer with a nanomechanical resonator exhibits a charge sensitivity of 1×10^{-4} charge of the electron.⁶ The displacement sensitivity of such a tiny device has almost reached quantum limits.^{2,12} A mass sensor based on the resonant frequency changes of a cantilever is also an attractive application due to its extreme sensitivity.¹³⁻¹⁸ Such a mass sensor will be possibly employed as a sensing component in future atom optics.¹⁹ An ion trapping technique has been widely studied due to the possibility of realizing quantum computation.²⁰ An ion trapping system with the integration of a nanomechanical device has been proposed.²¹ The coupling between qubits via nanomechanics is considered to provide a novel method to realize the entanglement of the internal state of ions. Such a coupling between nanomechanics and quantum systems including a quantum dot and superconducting quantum interferometer device (SQUID) will open up a novel realm in nanomechanics.²²

In this research, the ion detection based on resonant fre-

quency changes of a mechanical silicon resonator is demonstrated in vacuum. Low-energy ions from a mass filter are attached on the resonator, resulting in the decrease of the resonant frequency due to induced surface stress. Two kinds of silicon resonators were examined and their potential abilities are discussed.

II. FUNDAMENTALS OF ION DETECTION

We will briefly discuss the mass and ion sensing achieved by using a resonating sensor. Regarding the rectangle cantilever with a length, width, and thickness of l , w , and t , respectively, the resonant frequency can be approximated as follows:

$$f_0 = \frac{0.162t}{l^2} \sqrt{\frac{E}{\rho}}, \quad (1)$$

where E is the Young's modulus and ρ is the density.

Mass loading Δm is approximated by resonant frequencies f_0 and f' before and after mass loading:¹⁴

$$\Delta m = \frac{k}{4\pi^2} \left(\frac{1}{f'^2} - \frac{1}{f_0^2} \right). \quad (2)$$

Therefore, the resonant frequency after mass loading is given by

$$f' = \frac{1}{2\pi} \sqrt{\frac{k}{m_{\text{eff}} + \Delta m}}, \quad (3)$$

where m_{eff} is the effective mass of the cantilever.

If surface stress σ is generated only on one side of the cantilever and the mass loading can be ignored, the resonant frequency changes according to^{23,24}

^{a)} Author to whom correspondence should be addressed; electronic mail: tono@cc.mech.tohoku.ac.jp

$$f_{\text{stress}} = f_0 \sqrt{1 - \sigma(60l^2/14Et^3)}. \quad (4)$$

Compressive surface stress ($\sigma < 0$) increases the resonant frequency; in contrast, tensile stress decreases the resonant frequency.

Next we consider the electrostatic actuation of a cantilever in the case that a metal electrode opposed to the cantilever constructs a capacitance C with a gap distance d . Under the application of both dc voltage V_{dc} and ac voltage V_{ac} , the electrostatic force F_e is given as follows if the capacitive gap distance is supposed to be constant:

$$F_e = -\frac{\partial C}{\partial x}(V_{\text{dc}} + V_{\text{ac}})^2, \quad (5)$$

where x is the coordination vertical to the cantilever.

Suppose that the charges q_s are deposited on the cantilever. The total charges q_t are expressed as follows:

$$q_t = q_s + q_{\text{dc}} + q_{\text{ac}}, \quad (6)$$

where $q_{\text{dc}} = CV_{\text{dc}}$ and $q_{\text{ac}} = CV_{\text{ac}}$.

With this assumption, the electrostatic force F_c due to the charge is approximated as

$$F_c = -\frac{1}{4\pi\epsilon_0 d^2}(q_s q_{\text{dc}} + q_s q_{\text{ac}}), \quad (7)$$

where ϵ_0 is the dielectric constant of vacuum. If the deposited charges create a gradient field, the effective spring constant k' is given by

$$k' = k - \left\langle \frac{\partial F_c}{\partial z} \right\rangle. \quad (8)$$

Therefore, the resonant frequency changes as follows:

$$f' = \frac{1}{2\pi} \sqrt{\frac{k'}{m}}. \quad (9)$$

If the vibration amplitude of the cantilever is kept at a constant by feedback control via V_{dc} voltage, the change of the effective spring constant due to the charge deposition can be canceled and the resonant frequency change is negligible. Therefore, from the feedback voltage V_{dc} the deposited charges can be simply estimated.

III. EXPERIMENTAL SETUP

Figure 1 shows the schematic figure of the experimental setup.²⁵ A single-crystalline silicon cantilever^{26,27} was placed in a vacuum chamber and self-oscillated at a constant vibration amplitude. The rectangular single-crystalline silicon cantilevers were made from (100)-oriented silicon wafers. One cantilever (sample No. 1) as a resonator has a length, width, and thickness of 545, 163, and 0.50 μm , respectively. The calculated spring constant of the cantilever is 0.0053 N/m. The other cantilever (sample No. 2) has a length, width, and thickness of 60, 10, and 0.146 μm , respectively. The spring constant of the cantilever is calculated to be 0.006 N/m. An aluminum electrode for electrostatic actuation was placed near the cantilever. The cantilever was electrostatically oscillated by applying an ac voltage between the electrode and the cantilever, and its vibration was measured using a laser Doppler vibrometer via an optical win-

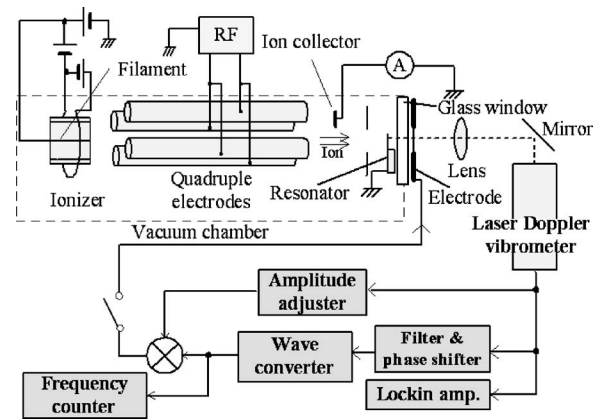


FIG. 1. Experimental setup for the measurement of mechanical response to ion attachment.

dow of the chamber.^{7,23} The output signal of the laser Doppler vibrometer was sent to the metal electrode via a phase shifter, filter, and wave converter, which self-oscillates the cantilever. In order to oscillate the cantilever at a constant amplitude, an amplitude adjuster consisting of a lock-in amplifier and a differential amplifier was employed in the feedback loop. The Q factor of the cantilever was measured from the decay curve of the vibration amplitude when the feedback loop was turned off and the amplitude was ringing down.²³ The oscillation frequency was measured using a frequency counter, and the vibration amplitude and ring-down curve were measured using a lock-in amplifier.

The cantilever was exposed to low-energy ions that were generated using an ionizer, in which electrons from a hot filament are accelerated by a grid electrode and ionized residual gases resulting from electron bombardment in a vacuum chamber. The vacuum chamber was pumped to a pressure of approximately 2×10^{-2} Pa using a turbomolecular pump. The generated ions are accelerated to the quadrupole electrodes with an acceleration voltage of 12 V, which acts as a mass filter. Depending on the frequency of the rf applied to the quadrupole electrodes, specific ions are filtered and attached to the cantilever. The ion flux density was monitored using an ion collector, and the value was calibrated to flux density at the cantilever. In front of the cantilever, an electrically shielded mesh electrode was placed in order to confirm that there was no electric field influence on the cantilever. Altering the current provided to the hot filament varied the ion density flux.

IV. EXPERIMENTS AND DISCUSSIONS

Low-energy pulsed ions through the quadrupole mass filter were attached on the self-oscillated cantilever (sample No. 1) and the mechanical responses were measured. Figure 2 shows the typical experimental result of the cantilever response when irradiating pulsed N_2 ions (N_2^+) with a peak height of 300 pA/cm^2 for a period of approximately 3 s. Figures 2(a)–2(d) show the oscillation frequency, amplitude of vibration, ion flux density, and driving gain, respectively. During the measurement, as shown in Fig. 2(b), the vibration amplitude was kept at a constant of 2.3 μm with the feedback control of the actuation voltage to the driving gain in

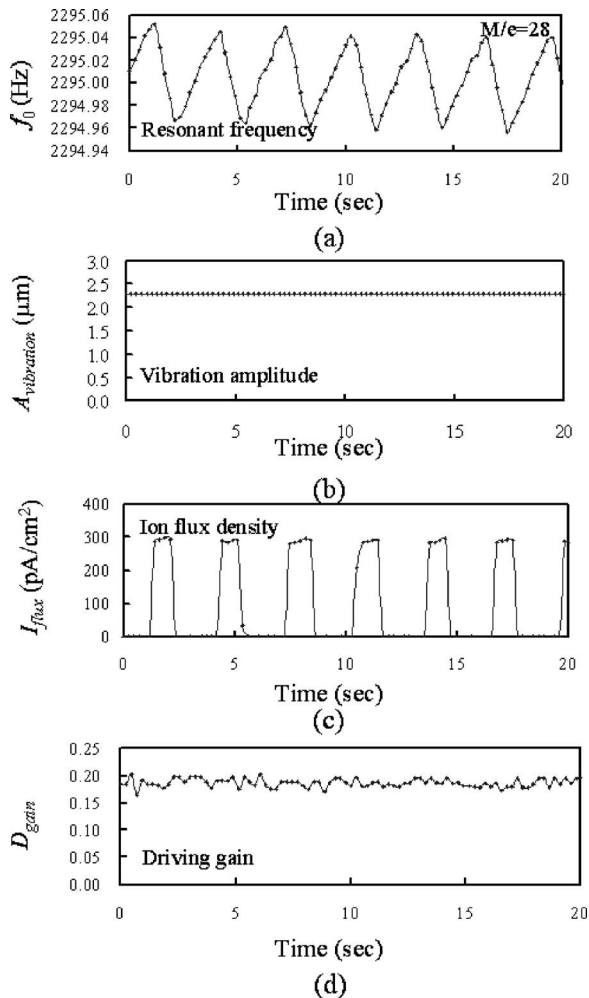


FIG. 2. Mechanical response to irradiation of N_2 ion pulses on the 500-nm-thick cantilever. (a) Frequency response. (b) Vibration amplitude during the measurement. (c) Irradiated ion pulses. (d) Driving gain of electrostatic actuation for keeping the amplitude a constant.

order to avoid the frequency changes that originated in the nonlinearity of the spring. Periodical frequency response according to the irradiation of the ion pulse could be observed as shown in Fig. 2(a). During exposure to the ion pulse, the resonant frequency was decreased due to ion attachment. In contrast, during pulse-off, the resonant frequency was monotonically increased due to the desorption of ion species. The value in Fig. 2(d) corresponds to the feedback gain, which exhibits a constant value. As discussed above, this feedback gain corresponds to the deposited charges on the native oxide of the silicon cantilever. Therefore, the surface charge density in the cycle of the ion attachment is considered to be a constant value.

Figure 3 shows the measurement result of hydrogen ion (H_2^+) attachment to the cantilever. In this measurement, the vibration amplitude was kept at $8 \mu\text{m}$ and ion pulses with peak heights of $4 \text{ pA}/\text{cm}^2$, as shown in Fig. 3(b), were irradiated to the cantilever. No remarkable periodic response could be found in the resonant frequency change. However, periodic behavior corresponding to ion pulses could be observed in the feedback gain. When hydrogen ions were attached to the cantilever, positive charges were deposited and

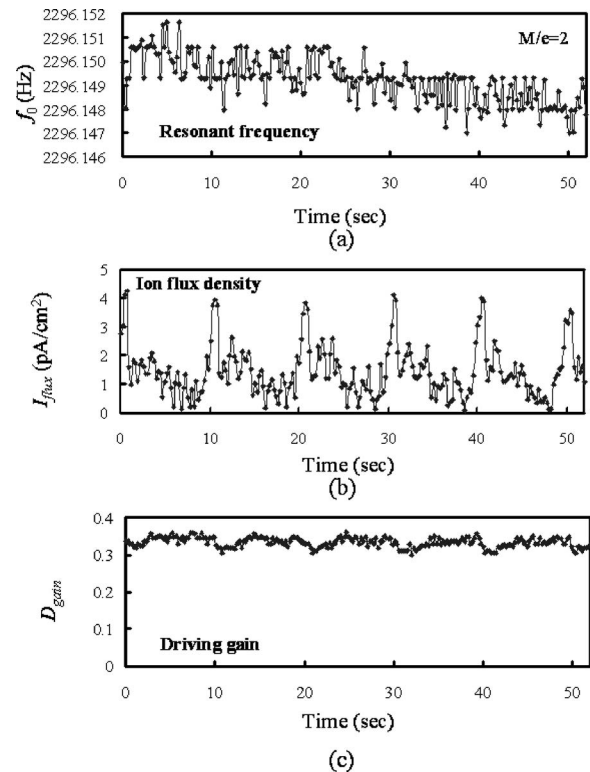


FIG. 3. Mechanical response to irradiation of hydrogen ion pulses on the 500-nm-thick cantilever. (a) Frequency response. (b) Irradiated ion pulses. (d) Driving gain of electrostatic actuation for keeping the amplitude a constant.

increased the driving force according to Eq. (7), thus the feedback gain decreased to keep the amplitude at a constant.

Next, a sequential experiment of different kinds of ion attachments was performed. Prior to this experiment, the cantilever surface was exposed to oxygen ions, which forms a Si-O-Si termination on the surface. Water ions (H_2O^+) with a flux density of $5\text{--}7 \text{ pA}/\text{cm}^2$ were irradiated to the silicon cantilever for 500 s. After a 1000-s interval, hydrogen ions (H_2^+) with a flux density of approximately $18 \text{ pA}/\text{cm}^2$ were irradiated to the cantilever for 450 s. The attachment of water ions decreased the resonant frequency by a 0.23 Hz due to mass loading of the water molecule. The oxidized surface (SiO_2) will be hydroxylated by a reaction with OH and H radicals generated from water ions, on which water molecules will be adsorbed. In this experiment, the Q factor of the cantilever was measured simultaneously, as shown in Fig. 4(c). It is interesting that the Q factor depends on the surface state created by attaching different ion species. The oxidized surface (Si-O) exhibits a high Q factor of approximately 20 000, and hydroxylation to (SiOH) lowers the Q factor down to 13 000. Details of the ion attachment effect on the Q factor will be published in elsewhere.²⁵

Next, the 146-nm-thick Si cantilever (cantilever No. 2) was employed to demonstrate the ion detection as well. This cantilever is thinner and smaller than that of cantilever No. 1 described above, and its spring constant of $0.006 \text{ N}/\text{m}$ is comparable to that of cantilever No. 1, which self-oscillated with a vibration amplitude of $0.3 \mu\text{m}$. The cantilever was exposed to the pulses of hydrogen ions (H_2^+) with a peak ion flux density of $65 \text{ pA}/\text{cm}^2$, as shown in Fig. 5. We could

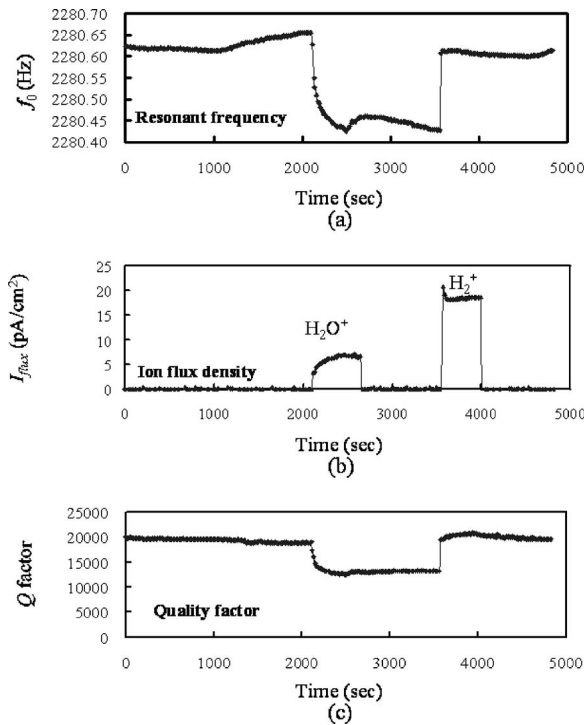


FIG. 4. Sequential irradiation of two kinds of ions: water ions and hydrogen ions, and its mechanical response on the 500-nm-thick cantilever. (a) Frequency response to ion attachment. (b) Ion pulse density. (c) Q factor of the resonator.

observe the periodic responses in frequency and feedback gain according to the pulse, as shown in Figs 5(a) and 5(c). Attachment of the ion pulse lowers the resonant frequency as well as the feedback gain.

In the following, we discuss the factor that causes the above response in ion attachment. In N_2 ion exposure, shown in Fig. 2, a frequency decrease of approximately 0.09 Hz was observed in a pulse irradiation with a peak ion density of 300 pA/cm^2 on the $0.5\text{-}\mu\text{m}$ -thick cantilever (sample No. 1). Supposing that mass loading decreases the frequency, the loaded mass can be calculated to be $2 \times 10^{-12} \text{ g}$ from Eq. (2). However, this calculated mass is unattainable due to the low ion flux density. The number of the irradiated N_2 ions is estimated to be approximately 1.7×10^6 ions/s. If all ions were attached on the surface, the surface density of adsorbed ions reaches 1.9×10^{-5} ions/nm. The mass loading speed is estimated to be only $7.7 \times 10^{-17} \text{ g/s}$, which is too small to explain the above experimental result. Therefore, the mass loading cannot be considered to be the main source of the resonant frequency change.

Another possibility is the frequency change due to the surface stress when ions are adsorbed on the surface. From Eq. (4) the stress variation due to the adsorption is calculated to be $1.3 \times 10^{-6} \text{ N/m}$ in the case where the resonant frequency decreased by 0.09 Hz. In these cantilevers, a thin native silicon dioxide exists on the surface, which exhibits compressive stress. Nitridation of silicon dioxide relaxes the compressive stress by approximately 0.3 N/m due to the formation of $\text{N-Si}_2\text{O}$ bonding on the entire surface.²⁸ The change of the observed frequency is qualitatively consistent with stress-induced frequency change.

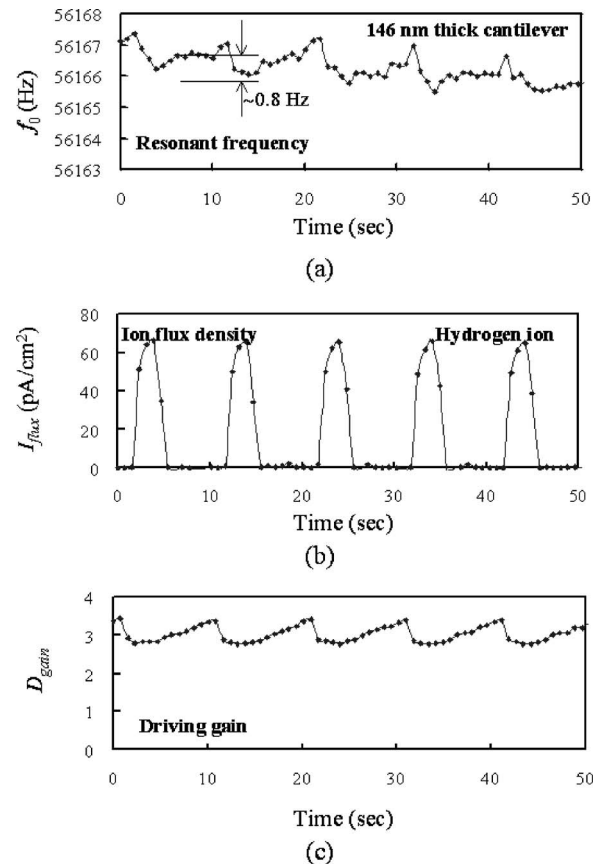


FIG. 5. Mechanical response to irradiation of hydrogen ion pulses on the 146-nm-thick cantilever. (a) Frequency response. (b) Irradiated ion pulses. (c) Driving gain of electrostatic actuation for keeping the amplitude a constant.

In contrast to the experiments on N_2 ion attachments, no resonant frequency response was observed on hydrogen ion attachment, as shown in Fig. 3(a). The influence of both loaded mass and surface stress on the frequency change was below the minimum limit of the detection. However, the driving gain to keep the amplitude a constant was varied according to ion irradiation, therefore, the positive charges are considered to deposit on the cantilever surface in hydrogen ion irradiation.

The attachment of water ions will hydroxylate the surface on the cantilever,²⁹ which relaxes the surface stress and reduces the resonant frequency, as can be seen in Fig. 4. The decrease of frequency due to water attachment is approximately 0.23 Hz. If the mass loading is dominant, the adsorbed mass is calculated to be 5.2 pg. However, this is much larger than that of irradiated ions as well. Meanwhile, if the surface stress is dominant, its value is calculated to be 0.016 N/m . The surface stress is considered as the main reason for the frequency change in either case. The mechanical Q factor is influenced by the surface state, as shown in Fig. 4(c). The creation and deactivation of energy dissipation sites on the surface causes the variation in the Q factor. In such cases, the change of the feedback control for the constant amplitude is influenced by both the deposited charges and the changes of the Q factor, which makes the estimation of the deposited charges difficult.

The smaller cantilever with a thickness of 146 nm

(sample No. 2) with a spring constant of 0.006 N/m exhibits a higher sensitivity to ion attachment, as the experiment on hydrogen ion attachment is shown in Fig. 5. In this case, the periodic frequency response to hydrogen attachment due to the surface stress could be observed as well, in which the cantilever was exposed to approximately 20 000 hydrogen ions per pulse. The mass of the 20 000 hydrogen ions is 6.9×10^{-20} g (69 Zg). The hydrogen ion attachment was found to deposit charges from the periodic response of the driving gain, and also slightly decreases the frequency by 0.8 Hz. The induced stress change is calculated to be 9.7×10^{-7} N/m.

ACKNOWLEDGMENTS

Part of this work was performed in the Venture Business Laboratory (VBL) of Tohoku University. This work was supported in part by a Grant-in Aid for Scientific Research from the Japanese Ministry of Education, Culture, Sports, Science and Technology of Japan.

¹K. L. Ekinci and M. L. Roukes, Rev. Sci. Instrum. **76**, 061101 (2005).

²A. Cho, Science **299**, 37 (2003).

³See, for example, *Scanning Tunneling Microscopy II*, edited by R. Wiesendanger and H.-J. Güntherodt (Springer, Berlin, 1992).

⁴H. J. Mamin and D. Rugar, Appl. Phys. Lett. **79**, 3358 (2001).

⁵R. H. Blick, A. Erbe, H. Krommer, A. Kraus, and J. P. Kotthaus, Physica E (Amsterdam) **6**, 821 (2000).

⁶A. N. Cleland and M. L. Roukes, Nature (London) **392**, 160 (1998).

⁷T. Ono and M. Esashi, Rev. Sci. Instrum. **74**, 5141 (2003).

⁸N. E. Jenkins, L. P. DeFlores, J. Allen, T. N. Ng, S. R. Garner, S. Kuehn, J. M. Dawlaty, and J. A. Marohn, J. Vac. Sci. Technol. B **22**, 909 (2004).

⁹N. V. Lavrik, M. J. Sepaniak, and P. G. Datskos, Rev. Sci. Instrum. **75**, 2229 (2004).

¹⁰Y. Arntz, J. D. Seelig, H. P. Lang, J. Zhang, P. Hunziker, J. P. Ramseyer, E. Meyer, and Ch. Gerber, Nanotechnology **14**, 86 (2003).

¹¹G. Li, L. W. Burggraf, and W. P. Baker, Appl. Phys. Lett. **76**, 1122 (2000).

¹²A. Gaidrzhy, G. Zolfagharkhani, R. L. Badzey, and P. Mohanty, Phys. Rev. Lett. **94**, 030402 (2005).

¹³Z. J. Davis, G. Abadal, O. Kuhn, O. Hansen, F. Grey, and A. Boisen, J. Vac. Sci. Technol. B **18**, 612 (2000).

¹⁴T. Ono, X. X. Li, H. Miyashita, and M. Esashi, Rev. Sci. Instrum. **74**, 1240 (2003).

¹⁵K. L. Ekinci, Y. T. Yang, and M. L. Roukes, J. Appl. Phys. **95**, 2682 (2004).

¹⁶S. Dohn, T. Sandberg, W. Svendsen, and A. Boisen, Appl. Phys. Lett. **86**, 233501 (2005).

¹⁷B. Llic, H. G. Craighead, S. Krylov, W. Senaratne, and C. Ober, J. Appl. Phys. **95**, 3694 (2004).

¹⁸A. Gupta, D. Akin, and R. Bashir, Appl. Phys. Lett. **84**, 1976 (2005).

¹⁹D. Meschede and H. Metcalf, J. Phys. D **36**, R17 (2003).

²⁰J. I. Cirac, and P. Zoller, Nature (London) **404**, 579 (2000).

²¹L. Tian and P. Zoller, Phys. Rev. Lett. **93**, 266403 (2004).

²²K. C. Schwab and M. L. Roukes, Phys. Today **205**, 36 (2005).

²³T. Ono, D. F. Wang, and M. Esashi, Appl. Phys. Lett. **83**, 1950 (2003).

²⁴S. Timoshenko, *Vibration Problems in Engineering*, 2nd ed. (Van Nostrand, New York, 1937).

²⁵T. Ono and M. Esashi, Appl. Phys. Lett. **87**, 044105-1 (2005).

²⁶J. Yang, T. Ono, and M. Esashi, Sens. Actuators B **82**, 102 (2000).

²⁷J. Yang, T. Ono, and M. Esashi, Appl. Phys. Lett. **77**, 3860 (2000).

²⁸A. N. Itakura, M. Shimoda, and M. Kitajima, Appl. Surf. Sci. **216**, 41 (2003).

²⁹O. Sneh, M. A. Cameron, and S. M. George, Surf. Sci. **364**, 61 (1996).